

Effect of manganese oxide on the densification and properties of ceria-doped scandia stabilized zirconia

C.K. Ng^{a,b}, S. Ramesh^{a,*}, C.Y. Tan^a, C.Y. Ching^a, N. Lwin^a and A. Muchtar^{c,d}

^aCenter of Advanced Manufacturing and Material Processing, Department of Mechanical Engineering, Faculty of Engineering, University of Malaya, 50603 Kuala Lumpur, Malaysia

^bDepartment of Materials Engineering, Faculty of Engineering & Built Environment, Tunku Abdul Rahman University College, Jalan Genting Kelang, 53300 Kuala Lumpur, Malaysia

^cFaculty of Engineering & Built Environment, Universiti Kebangsaan Malaysia, 43600 UKM Bangi, Selangor, Malaysia

^dFuel Cell Institute, Universiti Kebangsaan Malaysia, 43600 UKM Bangi, Selangor, Malaysia

In the present work, the effect of manganese oxide (MnO₂) additions (0, 0.5, 1 and 5 wt%) on the properties of ceria-doped scandia stabilized zirconia (10Sc1CeSZ) was investigated over the temperature range of 1400 °C to 1550 °C. The results showed that the addition up to 1 wt% had negligible effect on the mechanical properties of the ceramic. The samples containing up to 1 wt% MnO₂ attained above 97.5% relative density, Vickers hardness of 13–14 GPa and fracture toughness of about 3 MPam^{1/2}. In addition, it was revealed that the 0.5 wt% MnO₂ addition was beneficial in suppressing the cubic zirconia grain growth i.e. the highest average grain size was measured at 4.9 μm when sintered at 1550 °C as compared to 9.9 μm measured for the undoped zirconia when sintered at the same temperature. On the other hand, the addition of 5 wt% MnO₂ was found to be detrimental to the densification and properties of the zirconia, particularly when sintered at higher temperatures. This was attributed to the accelerated grain growth of the doped samples, i.e. the grain size increased by 2 fold, to 18.6 μm when sintered at 1550 °C.

Key words: Cubic Zirconia, Ceria-Doped Scandia Stabilized Zirconia, Manganese Oxide Addition, Sintering, Mechanical Properties.

Introduction

Solid oxide fuel cell (SOFC) is the most efficient high temperature fuel cell electric generators that can run on a variety of fuels, from hydrogen to hydrocarbon [1–5]. The high operating temperatures of SOFC enables natural gas fuels to be reformed within the cell and eliminate the need for an expensive external reformer. However, lowering the operating temperatures has significant impact on cost by allowing the use of cheaper interconnectors, gas manifolds and sealant materials. As a result, there has been huge interest in the development of new oxide ion electrolytes with improved performance for commercialization of SOFC technology [6–8].

Zirconia based ceramic has become an important electrolyte material for SOFC due to its excellent combination of good mechanical property and high ionic conductivity. The most common solid electrolyte material is yttria stabilized zirconia (YSZ) with a maximum bulk ionic conductivity of 0.1 S/cm recorded at 1000 °C [9–11]. In particular, scandia stabilized zirconia (ScSZ) is an alternative to YSZ for intermediate temperature SOFC

(600–800 °C). Scandia doping has been shown to result in high conductivities of 0.159 S/cm at 800 °C [12] and 0.32 S/cm at 1000 °C [13], thus exceeding that of YSZ at elevated temperatures.

One of the main limitations of oxide ion conductors as SOFC electrolytes is the undesirable phase transformation caused by impurities. It is reported that phase destabilization induced by manganese, boron, or silicon was observed in calcia/ yttria stabilized zirconia [14–17]. The manganese diffusion from the cathode took place during the heat treatment of cell fabrication in air; other impurities were found to be transferred from other components or processing equipment [14, 18]. These impurities were found to react with the stabilizers, leading to cubic phase destabilization and phase transformation into tetragonal symmetry. It is therefore important to investigate the reactions between electrolyte material and minor impurities.

The aim of this present work is to examine the effects of additions of different amount of MnO₂ on the densification, phase stability and mechanical properties of ceria-doped scandia stabilized zirconia (10Sc1CeSZ) ceramic.

Experimental

The as-received commercially available 1 mol% ceria-doped 10 mol% scandia stabilized zirconia (10Sc1CeSZ) powder was supplied by Daiichi, Japan. The powder had

*Corresponding author:
Tel : +603-7967-5209
Fax: +603-7967-7621
E-mail: ramesh79@um.edu.my

a total impurity concentration of less than 0.1 wt. %, comprised of small amount of various impurities (SiO_2 , Al_2O_3 , Fe_3O_4 , TiO_2 , Na_2O and CaO). The 10Sc1CeSZ powder had a specific surface area of $11.1 \text{ m}^2/\text{g}$ and an average particle size of $0.53 \mu\text{m}$. Varying amounts of high purity Manganese (IV) oxide (0.5, 1 and 5 wt. %) (R&M Chemicals, UK) were doped into the 10Sc1CeSZ powder by using ethanol as the mixing medium and subjected to attritor milling (Union Process Inc., USA) at 450 rpm for 1 hour with 2 mm diameter zirconia milling media. The slurry was filtered and dried in an oven at 60°C overnight. The dried cake was sieved using a $212 \mu\text{m}$ mesh sieve. Disc samples were prepared by uniaxial pressing at 5 MPa followed by cold isostatic pressing at 200 MPa. The pressed samples were sintered at various temperatures ranging from 1400°C to 1550°C for 2 hours at a heating rate of $10^\circ\text{C}/\text{min}$.

The specific surface area of all the powders was measured using the single point BET method on a Micrometrics (Tristar II) surface area analyzer under nitrogen gas. The phase analysis by X-ray diffraction (XRD) of the ceramics was carried out using a PANalytical Empyran XRD (The Netherlands) with CuK_α as the radiation source ($\lambda = 1.5406 \text{ \AA}$) operated at 45 kV, 40 mA, a step size of 0.02° over a $2\theta = 20^\circ - 80^\circ$. Microstructure characterization was performed by scanning electron microscopy (Phenom ProX SEM, The Netherlands) on polished and thermally etched sintered pellets. Grain size was determined by the line intercept technique using the SEM images.

The bulk density of the sintered samples was measured based on the Archimedes' principle using distilled water as immersion medium. Relative densities were calculated by taking the theoretical density of cubic zirconia as $5.74 \text{ g}/\text{cm}^3$ [19]. The Young modulus values were calculated based on the impulse excitation technique using a GrindoSonic's "MK5" sonic testing instrument (Belgium). Vickers hardness was obtained from polished sintered samples using an applied force of 98.1 N with a dwell time of 10 s. The indentation fracture toughness (K_{IC}) value was computed using the equation derived by Nihara et al. [20]:

Results and Discussion

The BET surface areas of the samples are summarized in Table 1. The results showed that all MnO_2 -doped powders showed higher specific surface area as compared to the undoped powder. The BET surface area was at a maximum of $12.88 \text{ m}^2/\text{g}$ for 0.5 wt% MnO_2 doped zirconia (i.e. 11.7% higher than the undoped ceramic), while the 1 and 5 wt% MnO_2 additions had produced specific surface area of ~ 3 to 4% higher than the undoped powder. This shows that the attritor milling was beneficial in reducing the particle size and hence preventing agglomeration from taking place.

Table 1. BET surface area of MnO_2 -doped 10Sc1CeSZ ceramics.

MnO_2 addition (wt%)	0	0.5	1	5
BET surface area (m^2/g)	11.53	12.88	11.84	11.97

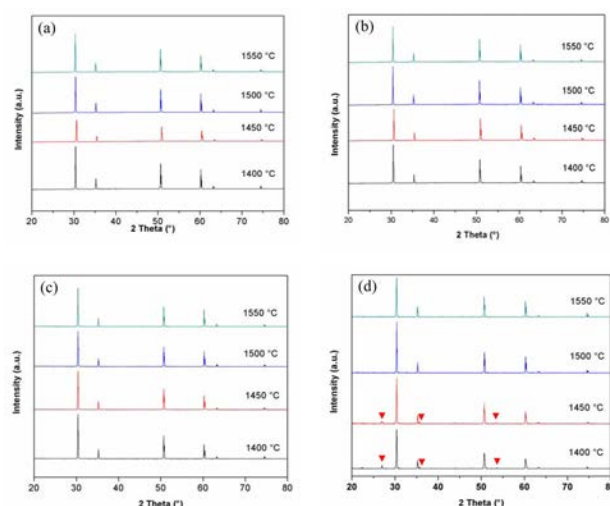


Fig. 1. The XRD plots of undoped and MnO_2 -doped 10Sc1CeSZ sintered samples: (a) undoped, (b) 0.5 wt% MnO_2 , (c) 1 wt% MnO_2 and (d) 5 wt% MnO_2 (All the unmarked peaks belong to that of cubic zirconia phase. The marked peaks shown for the 1400°C and 1450°C in (d) belongs to tetragonal peaks.)

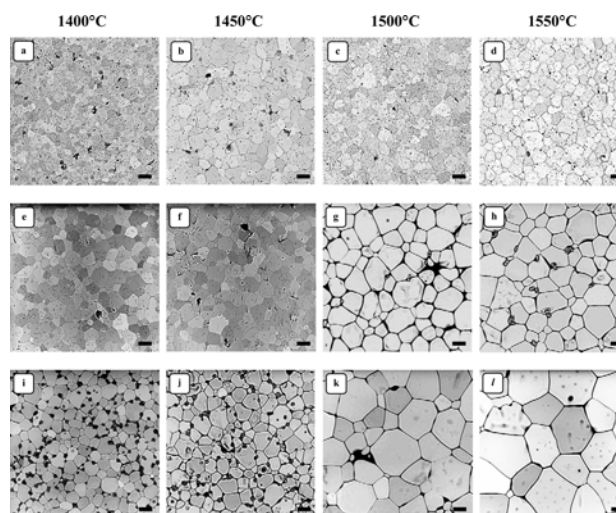


Fig. 2. Microstructural evolution of 0.5 wt% MnO_2 -doped (a to d), 1 wt% MnO_2 -doped (e to h) and 5 wt% MnO_2 -doped (i to l) 10Sc1CeSZ ceramics sintered at various temperatures. The value of the scale bar is $5 \mu\text{m}$.

The XRD plots of undoped and MnO_2 -doped 10Sc1CeSZ after sintering at 1400°C to 1550°C for 2 hours are shown in Fig. 1. The results indicated that all the XRD signatures for the undoped, 0.5 wt% MnO_2 -doped and 1 wt% MnO_2 -doped samples conformed to that of cubic zirconia phase (JCPDS file: 01-089-5485). In the case for the 5 wt% MnO_2 -doped sample sintered at 1400°C and 1450°C , there is three minor secondary

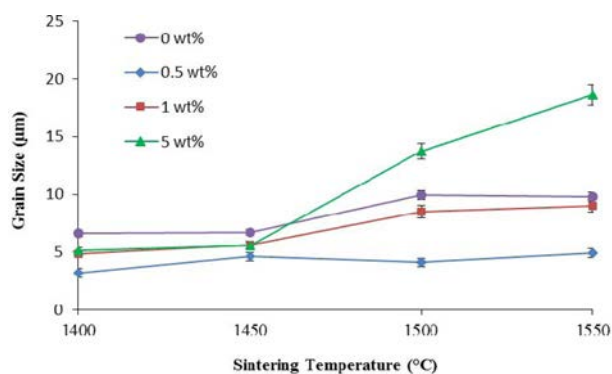


Fig. 3. The effect of sintering temperatures on the grain size of undoped (0 wt%) and MnO₂-doped 10Sc1CeSZ samples.

XRD peaks observed at $2\theta = 27^\circ$, 35.7° and 53.6° , believed to be that of the tetragonal zirconia phase (JCPDS file: 01-083-1376). However, the tetragonal zirconia phase was not detected for this sample when sintered $\geq 1500^\circ\text{C}$.

It has been reported in the literatures [21, 22] that high amount of manganese formed glassy liquid phase at grain boundaries and this could have played a role in destabilizing the cubic phase by drawing out minute amounts of scandia stabilizer from the cubic zirconia grains and hence promoting the formation of the tetragonal phase.

The microstructure evolution of the MnO₂-doped 10Sc1CeSZ samples sintered at 1400 °C to 1550 °C are shown in Fig. 2. The grain size calculated based on line intercept method as a function of sintering temperatures is presented in Fig. 3. For the undoped samples, the grain size was found to be about 6.7 µm when sintered at 1400-1450 °C, and subsequently the grains grew to about 9.9 µm when the sintering temperature increased to 1500-1550 °C. On the other hand, the grain sizes of the 0.5 wt% and 1 wt% MnO₂ additions samples were found to be smaller than the undoped sample i.e. 4.9 µm and 9.0 µm recorded for samples sintered at 1550 °C, respectively. In contrast, for the 5 wt% MnO₂-doped sample, the microstructure developed in a similar way to that of the undoped samples up to 1450 °C, however as the sintering temperature was increased this was accompanied by a rapid grain growth as shown in Fig. 3. The average grain sizes measured for this sample were 13.7 µm and 18.6 µm when sintered at 1500 °C to 1550 °C, respectively.

The variation of relative density of sintered ceramics with increasing sintering temperatures is shown in Fig. 4. The results indicated that the undoped and up to 1 wt% MnO₂-doped samples were able to attain above 97.5% relative density, while the 5 wt% MnO₂-doped zirconia exhibited a lower relative density, about 95%, when sintered at 1400 °C, and subsequently declined to 92% when sintered at 1550 °C. This observation is in good agreement with the other researchers [23-26] who reported that the incorporation of MnO₂ in yttria stabilized

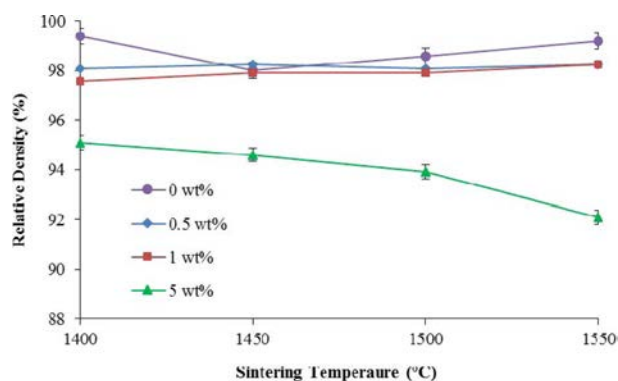


Fig. 4. The variation of relative density with increasing sintering temperatures for the undoped (0 wt%) and MnO₂-doped 10Sc1CeSZ samples.

zirconia was beneficial in promoting densification at lower sintering temperatures (1250-1300 °C) and may be detrimental to densification when fired at higher sintering temperatures (above 1400 °C). On the other hand, the lower relative density exhibited by the 5 wt% MnO₂-doped 10Sc1CeSZ throughout the sintering temperatures experimented could be attributed to the presence of large amount of residual pores located mainly at grain boundary regions, believed to be associated with the melting of large amount of manganese oxide especially at higher sintering temperatures as observed in the SEM micrographs shown in Fig. 2.

The effect of temperatures and dopants on the Vickers hardness, fracture toughness, and elastic modulus of the sintered 10Sc1CeSZ samples are presented in Fig. 5 to Fig. 7. The mechanical property trends correlated well with the relative density shown in Fig. 4. It has been found that for undoped and up to 1 wt% MnO₂-doped 10Sc1CeSZ, the Vickers hardness (12.6-13.9 GPa) and fracture toughness ($\sim 3 \text{ MPam}^{1/2}$) did not vary significantly with increasing temperatures, while the elastic modulus fluctuated within the range of 169 and 206 GPa. This results showed that the mechanical stability of scandia stabilized zirconia ceramic was not affected by the incorporation of up to 1 wt% of MnO₂, compared to the observation reported in by several researchers for up to 1 wt% MnO₂ addition in Y-TZP ceramic [22, 25, 27]. On the other hand, in the case of 5 wt% MnO₂-doped samples, the fracture toughness and Vickers hardness were observed to be lower when compared to the undoped ceramic. The 5 wt% Mn-doped zirconia exhibited low hardness of about 12 GPa when sintered between 1400-1450°C, before decreasing further with sintering, down to 10.5 GPa when sintered at 1550 °C. The fracture toughness was found to be about 2.8-2.9 MPam^{1/2} when sintered between 1400-1500°C, and subsequently decrease to 2.5 MPam^{1/2} at 1550 °C. Similarly, the elastic modulus of this sample as shown in Fig. 7 revealed a decreasing trend with increasing sintering temperature and attained a low value of 143 GPa at 1550 °C. This decline in the mechanical

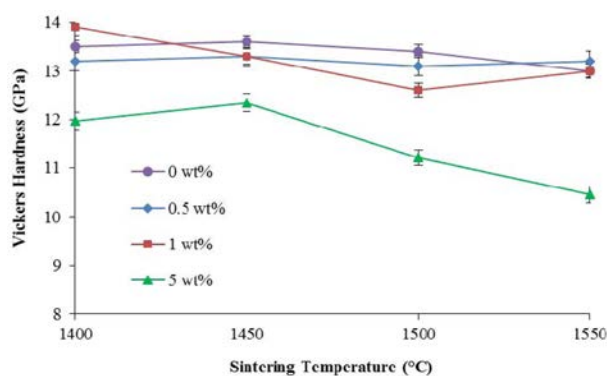


Fig. 5. The effect of sintering temperatures on the Vickers hardness of undoped (0 wt%) and MnO₂-doped 10Sc1CeSZ samples.

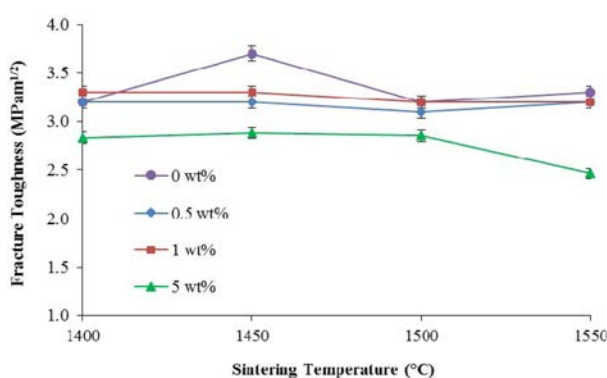


Fig. 6. The effect of sintering temperatures on the fracture toughness of undoped (0 wt%) and MnO₂-doped 10Sc1CeSZ samples.

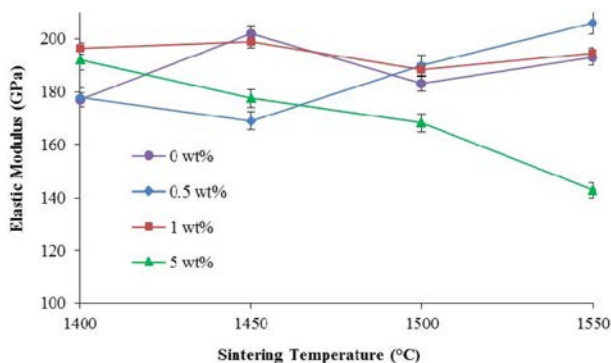


Fig. 7. The effect of sintering temperatures on the elastic modulus of undoped (0 wt%) and MnO₂-doped 10Sc1CeSZ samples.

properties is believed to be associated with grain growth when sintered at higher temperatures.

Conclusions

The effect of manganese oxide addition on the sinterability of ceria-doped scandia stabilized zirconia (10Sc1CeSZ) was investigated over the temperature range of 1400 °C to 1550 °C. The results indicated that the additions of up to 1 wt% MnO₂ was beneficial in suppressing the grain growth of cubic zirconia without

affecting the mechanical properties of the ceramic. The cubic phase stability was not disrupted with lower dopant contents of up to 1 wt% MnO₂ throughout the sintering regime employed. Nevertheless, the addition of high amount of manganese (5 wt%) was found to be detrimental as it affected the cubic phase stability of the zirconia matrix and resulted in grain growth when sintered at higher temperatures. This was also accompanied by deterioration of the Vickers hardness, fracture toughness and elastic modulus.

Acknowledgments

This study was supported under the PPP grant number PG080-2013A, UMRG grant number RP024B-13AET and Esciencefund grant number SF010-2014. The authors gratefully acknowledge University of Malaya and the Ministry of Science, Technology & Innovation for the financial support.

References

1. B.C. Steele, A. Heinzl, *Nature* 414 (2001) 345-352.
2. A.B. Stambouli and E. Traversa, *Renewable and Sustainable Energy Reviews* 6 (2002) 433-455.
3. S.M. Haile, *Acta Materialia* 51 (2003) 5981-6000.
4. S. McIntosh and R.J. Gorte, *Chemical Reviews* 104 (2004) 4845-4866.
5. F. Krok, I. Abrahams, W. Wrobel, A. Kozanecka-Szmigiel and J.R. Dygas, *Mater. Sci.-Poland* 24 (2006) 13-22.
6. R.M. Ormerod, *Chem. Soc. Rev.* 32 (2003) 17-28.
7. A.J. Jacobson, *Chem. Mater.* 22 (2009) 660-674.
8. A. Orera and P.R. Slater, *Chem. Mater.* 22 (2009) 675-690.
9. S. C. Singhal, *Solid State Ionics* 135 (2000) 305-313.
10. S.P.S. Badwal and K. Foger, *Ceram. Inter.* 22 (1996) 257-265.
11. H. Yokokawa, N. Sakai, T. Horita and K. Yamaji, *Fuel cells* 1 (2001) 117-131.
12. D. Lee, I. Lee, Y. Jeon and R. Song, *Solid State Ionics* 176 (2005) 1021-1025.
13. S.P.S. Badwal, *J. Mater. Sci.* 22 (1987) 4125-4132.
14. M.K. Mahapatra, P. Singh and S.T. Misture, *Appl. Phys. Lett.* 101 (2012) 131606.
15. N.M. Beekmans and L. Heyne, *Electrochimica Acta* 21 (1976) 303-310.
16. D.Z. De Florio and R. Muccillo, *Mater. Res. Bull.* 39 (2004) 1539-1548.
17. H. Kishimoto, N. Sakai, K. Yamaji, T. Horita, Y.P. Xiong, M.E. Brito and H. Yokokawa, *J. Mater. Sci.* 44 (2009) 639-646.
18. M. Shimazu, T. Isobe, S. Ando, K.I. Hiwatashi, A. Ueno, K. Yamaji, H. Kishimoto, H. Yokokawa, A. Nakajima and K. Okada, *Solid State Ionics* 182 (2011) 120-126.
19. H. P. Dasari, J. S. Ahn, K. Ahn, S.-Y. Park, J. Hong, H. Kim, K. J. Yoon, J.-W. Son, H.-W. Lee and J.-H. Lee, *Solid State Ionics* 263 (2014) 103-109.
20. K. Niihara, R. Morena and D. P. H. Hasselman, *J. Mater. Sci. Lett.* 1 (1982) 13-16.
21. T. Zhang, L. Kong, Z. Zeng, H. Huang, P. Hing, Z. Xia and J. Kilner, *J. Solid State Electrochem.* 7 (2003) 348-354.
22. S. Ramesh, W.J. Kelvin Chew, C.Y. Tan, J. Purbolaksono, A.M. Noor, M.A. Hassan, U. Sutharsini, M. Satgunam and W.D. Teng, *Ceram. Silikat* 57 (2013) 28-32.

23. M. M. Khan, S. Ramesh, L. T. Bang, Y. H. Wong, S. Ubenthiran, C. Y. Tan, J. Purbolaksono and H. Misran, *J. Mater. Eng. Perform.* 23 (2014) 4328-4335.
24. M.K. Manoj, N. Li, V. Atul and P. Singh, *Solid State Ionics* 253 (2013) 223-226.
25. S. Ramesh, S. Meenaloshini, C.Y. Tan, W.J. Kelvin Chew and W.D. Teng, *Ceram. Inter.* 34 (2008) 1603-1608.
26. S. Ramesh, M. Amiriyani, S. Meenaloshini, R. Tolouei, M. Hamdi, J. Pruboloksono and W. D. Teng, *Ceram. Inter.* 37 (2011) 3583-3590.
27. S. M. Kwa, S. Ramesh, L.T. Bang, Y.H. Wong, W.J. Chew, C.Y. Tan, J. Purbolaksono, H. Misran, and W.D. Teng, *J. Ceram. Proc. Res.* 16 (2015) 193-198.